



# Performance of visual, manual, and automatic coronary calcium scoring of cardiac $^{13}\text{N}$ -ammonia PET/low dose CT

Magdalena M. Dobrolinska, MD,<sup>a</sup> Sergiy V. Lazarenko, PhD,<sup>b</sup> Friso M. van der Zant, MD, PhD,<sup>b</sup> Lonneke Does, BSc,<sup>b</sup> Niels van der Werf, MSc,<sup>c,d</sup> Niek H. J. Prakken, MD, PhD,<sup>a</sup> Marcel J. W. Greuter, PhD,<sup>a,e</sup> Riemer H. J. A. Slart, MD, PhD,<sup>a,f</sup> and Remco J. J. Knol, MD, PhD<sup>b</sup>

<sup>a</sup> Medical Imaging Center, Departments of Radiology, Nuclear Medicine and Molecular Imaging, University of Groningen, University Medical Center Groningen, Groningen, The Netherlands

<sup>b</sup> Department of Nuclear Medicine, Northwest Clinics, Alkmaar, The Netherlands

<sup>c</sup> Department of Radiology, University of Utrecht, University Medical Center Utrecht, Utrecht, The Netherlands

<sup>d</sup> Department of Radiology & Nuclear Medicine, Erasmus University Medical Center Rotterdam, Rotterdam, The Netherlands

<sup>e</sup> Department of Robotics and Mechatronics, Faculty of Electrical Engineering, Mathematics & Computer Science, University of Twente, Enschede, The Netherlands

<sup>f</sup> Department of Biomedical Photonic Imaging, Faculty of Science and Technology, University of Twente, Enschede, The Netherlands

Received Feb 9, 2022; accepted Apr 29, 2022

doi:10.1007/s12350-022-03018-0

**Background.** Coronary artery calcium is a well-known predictor of major adverse cardiac events and is usually scored manually from dedicated, ECG-triggered calcium scoring CT (CSCT) scans. In clinical practice, a myocardial perfusion PET scan is accompanied by a non-ECG triggered low dose CT (LDCT) scan. In this study, we investigated the accuracy of patients' cardiovascular risk categorisation based on manual, visual, and automatic AI calcium scoring using the LDCT scan.

**Methods.** We retrospectively enrolled 213 patients. Each patient received a  $^{13}\text{N}$ -ammonia PET scan, an LDCT scan, and a CSCT scan as the gold standard. All LDCT and CSCT scans were scored manually, visually, and automatically. For the manual scoring, we used vendor recommended software (Syngo.via, Siemens). For visual scoring a 6-points risk scale was used (0; 1-10; 11-100; 101-400; 401-100; > 1 000 Agatston score). The automatic scoring was performed with deep learning software (Syngo.via, Siemens). All manual and automatic Agatston scores were converted to the 6-point risk scale. Manual CSCT scoring was used as a reference.

**Results.** The agreement of manual and automatic LDCT scoring with the reference was low [weighted kappa 0.59 (95% CI 0.53-0.65); 0.50 (95% CI 0.44-0.56), respectively], but the

**Supplementary Information** The online version contains supplementary material available at <https://doi.org/10.1007/s12350-022-03018-0>.

The authors of this article have provided a PowerPoint file, available for download at SpringerLink, which summarises the contents of the paper and is free for re-use at meetings and presentations. Search for the article DOI on SpringerLink.com.

**Funding** M.M.D. received the "EACVI Research Grant 2020" and "Specialised Research Fellowship 2019 Grant from "Club 30" and Polish Cardiac Society".

Magdalena M. Dobrolinska and Sergiy V. Lazarenko have equal contribution.

Reprint requests: Magdalena M. Dobrolinska, MD, Medical Imaging Center, Departments of Radiology, Nuclear Medicine and Molecular Imaging, University of Groningen, University Medical Center Groningen, 9700 RB Groningen, The Netherlands; [magdalena.dobrolinska@gmail.com](mailto:magdalena.dobrolinska@gmail.com)

J Nucl Cardiol 2023;30:239–50.

1071-3581/\$34.00

Copyright © 2022 The Author(s)

agreement of visual LDCT scoring was strong [0.82 (95% CI 0.77-0.86)].

**Conclusions.** Compared with the gold standard manual CSCT scoring, visual LDCT scoring outperformed manual LDCT and automatic LDCT scoring. (J Nucl Cardiol 2023;30:239–50.)

**Key Words:** CAD • PET • CT • Image interpretation

#### Abbreviations

CAC	Coronary artery calcium
CSCT	Calcium scoring CT scan
LDCT	Low dose CT scan
AI	Artificial Intelligence

**See related editorial, pp. 251–253**

## INTRODUCTION

Coronary artery calcium (CAC) score is not only a sign of atherosclerotic processes, but also a well-known risk predictor of cardiovascular diseases (CVD) for asymptomatic individuals with an intermediate risk of significant coronary artery stenosis.<sup>1</sup> A higher CAC score has shown to be associated with a higher risk of atherosclerotic disease.<sup>2,3</sup> Particularly, individuals with CAC > 100 experience more cardiovascular events, as compared to those with lower CAC scores.<sup>4</sup> Furthermore, Peng et al showed that the probability of a cardiovascular event even increases when the CAC score exceeds 1 000.<sup>5</sup> Conversely, the absence of coronary calcium is considered to be the most important negative marker of CVD.<sup>6</sup> However, the value of CAC scoring is not limited to asymptomatic individuals. Lo-Kioeng-Shioe et al demonstrated that CAC scoring also adds value to the prediction of major adverse cardiac events (MACE) in symptomatic patients.<sup>7</sup>

Traditionally, CAC score is calculated from dedicated, ECG-triggered coronary calcium scoring computed tomography (CSCT) scans following the standard manual Agatston scoring method.<sup>8</sup> The alternatives for time consuming manual calcium scoring are visual and automatic scoring methods. Visual scoring typically categorizes visible CAC by eye balling in one of six groups.<sup>9</sup> This method has been described in the past decade and is known to have good agreement with the gold standard, CSCT scans.<sup>9</sup> Recently, new commercially available software has emerged, which employs deep learning methods (DL) to calculate the Agatston score. DL enables automatic calcium scoring, and was previously validated on CSCT scans.<sup>10</sup>

In everyday clinical practice, myocardial perfusion imaging (MPI) positron emission tomography (PET) is preceded by non-ECG triggered low dose CT (LDCT) scans instead of CSCT scans. The LDCTs are used for attenuation correction of the PET data. Importantly,

accurate assessment of CAC from LDCT scans would certainly add new information about patients' risk to the results of MPI. Besides standard non-contrast coronary calcium scoring scans, it was demonstrated that coronary calcium scoring is feasible on almost all diagnostic non-contrast chest CT scans.<sup>11</sup> As underlined in Society of Cardiovascular Computed Tomography and Society of Thoracic Radiology (SCCT/STR) guidelines, calcium scores derived from LDCT scans should be reported, although there is still insufficient evidence on which method to use.<sup>12</sup> In this study we therefore decided to use an automatic, clinically available method based on deep learning to measure CAC from LDCT and CSCT scans. In addition, we assessed all LDCT and CSCT scans both visually and manually. The aim of the present study is to compare automatic, manual, and visual coronary calcium scoring performance from LDCT scans acquired during cardiac <sup>13</sup>N-ammonia PET/CT against manual scoring from dedicated CSCT scans as the gold standard.

## METHODS

### Patients

In this single center, retrospective study we included patients who underwent a <sup>13</sup>N-ammonia-PET/LDCT and a dedicated CSCT scan between 2013 and 2019. All included patients suffered from angina, chest pain, dyspnea, or were suspected of or had known CAD. Each <sup>13</sup>N-ammonia-PET scan was preceded by CSCT scan, which was typically followed by CCTA. The decision whether or not to proceed with ammonia-PET was made by cardiologist based on CSCT and/or CCTA results, the patient's symptoms, and patient's risk group. The time between both scans did not exceed 6 months to minimize any individual changes in calcium scores. Patient exclusion criteria were: myocardial infarction, previous percutaneous coronary intervention (PCI), or PCI between CSCT and <sup>13</sup>N-ammonia-PET MPI. The study was approved by the local scientific board, and the need to receive approval from the local medical ethical review committee was waived since the study was not within the scope of the Dutch Medical Research Involving Human Subjects Act (section 1.b; February 26, 1998). Additionally, as a standard procedure at the Department of Nuclear Medicine of the Northwest Clinics, all included patients gave written consent to the use of their anonymized data for scientific purposes.

## Data acquisition

**CSCT protocol** Relevant CSCT data acquisition parameters are presented in Table 1. CSCT scans were prospectively ECG-triggered at 60% of R-R interval without radiocontrast, and during inspiratory breath-hold. A dual source  $2 \times 64$  detector CT system with flying focal spot was used (Somatom Definition Flash, Siemens Healthineers, Forchheim, Germany) at a tube voltage of 120 kVp. The dataset was reconstructed using a B35f medium kernel at 3 mm slice thickness with an increment of 1.5 mm.

**LDCT protocol** LDCT scans were acquired on a PET/CT system (Biograph-16 TruePoint, Siemens Healthineers, Forchheim, Germany) and performed prior to the  $^{13}\text{N}$ -ammonia-PET MPI study to serve as attenuation correction CT. LDCT scans were non-ECG-triggered, non-contrast without inspiratory breath-hold. All patients were scanned at 130 kVp. Images were reconstructed with standard filtered back projection using a B31s kernel at 3 mm slice thickness and 1.5 mm increment (Table 1).

## Phantom study

In addition, an anthropomorphic thoracic phantom (QRM Thorax phantom, PTW, Germany) with a large calibration insert of hydroxyapatite ( $200 \text{ mg/cm}^3$ , QRM CCI, PTW, Germany) was scanned with the CSCT and LDCT protocols to determine the calcium detection threshold at 130 kVp (Figure 1), following the method of Thomas et al,<sup>13</sup> described in the equation below. Each protocol was scanned five times and the mean CT value of the large calibration rod was determined within a

large region of interest within the central slice. The recalculated calcium HU threshold played no role in the deep learning algorithm as it was trained and validated on 130 kVp data.<sup>10</sup>

$$t_{130\text{kVp}} = 130\text{HU} \times \frac{\text{HU}_{\text{CaHA}@130\text{kVp}}}{\text{HU}_{\text{CaHA}@120\text{kVp}}}$$

$t_{130\text{kVp}}$  = adapted threshold at 130 kVp,  $\text{HU}_{\text{CaHA}@130\text{kVp}}$ —HU value of calcium insert scanned at 130 kVp,  $\text{HU}_{\text{CaHA}@120\text{kVp}}$ —HU value of calcium insert scanned at 120 kVp

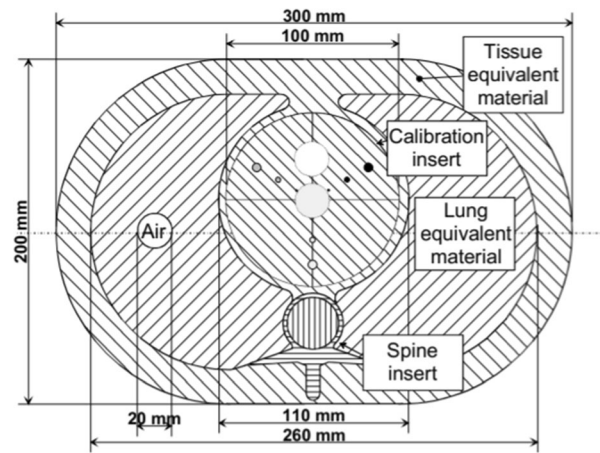


**Figure 1.** Overview of an anthropomorphic thorax phantom with calcium inserts.

**Table 1.** Acquisition and reconstruction parameters for CSCT and LDCT scans

	CSCT	LDCT
Scanner	Somatom Definition Flash, Siemens Healthcare	Biograph TruePoint, Siemens Healthcare
Tube voltage (kVp)	120	130
Qref. mAs	80	25
Field of view	228	500
Collimation (mm)	$2 \times 64 \times 1.2$	$16 \times 1.2$
Rotation time (s)	0.285	0.6
Kernel	B35f	B31s
Mode	Spiral	Spiral
Slice thickness	3.0	3.0
Pitch	3.2	0.95
Increment	1.5	3.0
$\text{CTDI}_{\text{vol}}$ (mGy)	1.3	2.8

## Scoring methods

Both LDCT and CSCT scans were transferred to a workstation (Syngo.via, Siemens Healthineers, Forchheim, Germany) for CAC analysis. All scans were scored visually, manually, and automatically on axial images for each separate artery (LM—left main, LAD—left anterior descending, RCA—right coronary artery, LCx—left circumflex artery) and as a total calcium score. In a per vessel analysis, LM and LAD were taken together as one single vessel.

**Manual scoring** Manual scoring of CSCT scans was done according to the Agatston method in which calcium is defined by a threshold of 130 HU and an area  $\geq 1 \text{ mm}^2$ .<sup>8</sup> For the manual LDCT scoring, the tube voltage corrected threshold was used. Manual scoring was performed by two observers (L.D. and M.M.D.) using dedicated software (syngo.via CT CaScoring VB50, Siemens Healthineers, Forchheim, Germany).

**Automatic scoring** The automatic scoring for LDCT and CSCT was performed with a commercially available algorithm, the details of which were explained previously.<sup>10</sup> In short, the calcium scoring software (syngo.via CT CaScoring VB50, Siemens Healthineers, Forchheim, Germany) uses deep learning methods to determine the calcium score.<sup>10</sup> It detects calcium containing voxels which exceed the threshold of 130 HU and assigns them to labeled coronary arteries. First, the heart was segmented with a U-Net architecture from the CT volume. Next, the CT volume was cropped to the heart and the coronary map was registered. Finally, a CNN network was applied to mask coronary arteries. As a result, the Agatston score was calculated on a per vessel basis and also as a global Agatston score for the entire coronary tree.<sup>10</sup>

**Visual scoring** For visual scoring of LDCT and CSCT scans we employed the previously described 6-point patient risk scale (Table 2).<sup>9</sup> Visual scoring was performed twice by one observer (M.M.D.) blinded to the results of the gold standard CSCT.

## Statistical analysis

Continuous variables were presented as means (with standard deviations or 95% confidence intervals) or medians (with interquartile range, IQR). Normality of variables was visually assessed based on histograms and q-q plots. Spearman's correlation was used to calculate correlations between manual and automatic scores. Total and per-vessel manual and automatic methods scores were compared to the gold standard using Bland–

Altman plots. For the comparison of non-parametric data, the Wilcoxon signed rank test was used. All manually and automatically measured scores were converted into the six risk groups. The agreement in risk group classification between the different scoring methods was measured using a Cohen weighted linear  $\kappa$  with 95% confidence intervals (95% CI). The kappa coefficients were categorized as: 0.01-0.2: slight agreement, 0.21-0.4: fair agreement, 0.41-0.6: moderate agreement, 0.61-0.8: substantial agreement, and 0.81-0.99 excellent agreement.<sup>14</sup> An Agatston score of  $\geq 1$  was defined as CAC positive. The sensitivity, specificity, positive predictive value (PPV) and negative predictive value (NPV) of CAC detection on LDCT scans was calculated.<sup>15</sup> A *P* value  $< 0.05$  was considered statistically significant. Statistical analyses were performed with Statistical Package for the Social Sciences (SPSS v 23; IBM, Armonk, NY) and MedCalc (MedCalc 15.8, MedCalc Software).

## RESULTS

### Phantom results

The average CT-value of the calibration insert was 249 and 269 HU, at 130 kVp and 120 kVp, respectively. The calcium HU threshold for a tube voltage of 130 kVp was calculated at 123 HU.

### Patients' characteristics

In total, 213 patients met the inclusion criteria, 111 (52.4%) were men. Mean patients' age was  $64 \pm 9$  years. Median time between LDCT and CSCT scans was 4 (2.0, 4.0) weeks. The available clinical information of 174 out of 213 study participants is summarized in Table 3. Agatston score results from CSCT scans are shown in Table 4.

### Automatic, visual, and manual scoring of CAC from CSCT scans

**CSCT calcium score analysis** *Total manual agatston score vs automatic scoring* The median value of total Agatston score was similar for the manual and automatic scoring methods: 579.4 (IQR 139.4, 1103.8) and 589.9 (IQR 129.1, 1100.3), respectively. The median difference between manual and automatic Agatston score measured from CSCT scans was 1.4 (95% CI  $-0.1$ -11.45) (Figure 2A). There was an excellent correlation between manual and automatic methods

( $r = 0.99$ ;  $P < .001$ ). The agreement between manual and automatic Agatston score risk group classification was excellent ( $\kappa = 0.95$ , 95% CI 0.92-0.97) (Table 5, Supplementary Table S1). 91% scans were assigned to the same category. Based on manual scoring from CSCT scan, 5.6% of the included patients had an Agatston

score of zero. Based on the automatic method, 0.9% of scans was incorrectly assigned to the zero Agatston score group (Table 5, Supplementary Table S1).

**Total manual Agatston score vs visual scoring** The agreement of risk group classification between manual and visual Agatston score was excellent ( $\kappa = 0.88$ , 95% CI 0.85-0.92). 82.1% of scans were within the same category. Based on visual analysis, none of the scans was misclassified into the zero Agatston score group (Table 5).

**Table 2.** The description of visual 6-point scale which was used for visual calcium scoring

Visual six-point scale	Agatston score equivalent
0	0
1	1-10
2	11-100
3	101-400
4	401-1 000
5	> 1 000

**Automatic, visual, and manual scoring of CAC from LDCT scans**

**LDCT calcium score analysis** *Automatic assessment from LDCT vs gold standard* The total Agatston score automatically derived from LDCT scans was significantly lower compared to that of CSCT scans (206.9 (IQR 20.5, 492.1) vs. 579.4 (IQR 139.4, 1103.8);  $P < .001$ ). Correlation between two scores was excellent ( $r = 0.93$ ;  $0 < 0.001$ ). The median difference between

**Table 3.** Baseline characteristics of study participants, myocardial

	Total n = 174/213	Male 54.6%	Female 45.4%
Age (y)	61.7 ± 9.3	60.4 ± 8.8	63.1 ± 9.7
BMI	27.9 ± 4.4	27.3 ± 4.1	28.7 ± 4.7
Risk factors			
Positive family history (%)	44.4	39.1	50.6
Smoking (%)	17	15.2	18.9
Diabetes (%)*	9.4	12.0	6.3
Hypercholesterolemia (%)	39.2	35.9	43.0
Hypertension (%)	51.5	41.3	63.3
Previous cardiac events			
Previous MI (%)	0.6	1.1	0
Previous PCI (%)	2.3	3.3	1.3
Previous CABG (%)	0.6	1.1	0
Duke Clinical Score <sup>28</sup>	40.0 ± 26.1	52.6 ± 24.4	26.5 ± 20.7
Cardiac medication			
None (%)	10.2	8.9	11.7
Statins (%)	71.9	73.3	70.1
Anticoagulants (%)	65.9	70.0	61.0
Betablocker (%)	55.7	54.4	57.1
Calcium antagonist (%)	16.8	21.1	11.7
AT2-antagonist or ACE-inhibitor (%)	32.9	31.1	35.1
Diuretics (%)	12.0	10.0	14.3
Nitrates (%)	5.4	5.6	5.2

Table summarizes clinical information about available 174 out of 213 patients. Values are presented as% or means (± SD) of 174/213 patients, due to limited availability.

CABG coronary artery bypass grafting; MI myocardial infarction; PCI percutaneous coronary intervention

\*Diabetes Type I and Type II



**Table 4.** Results of baseline CSCT scan

	<b>Baseline characteristics</b>
CAC categories based on Agatston score from CSCT scans	
0	12 (5.6%)
1	9 (4.2%)
2	27 (12.7%)
3	34 (16.0%)
4	69 (32.4%)
5	62 (29.1%)
Agatston score from CSCT scans	
CAC total	579.4 (139.4, 1103.85)
CAC LM	0.0 (0.0, 30.5)
CAC LAD	269.4 (73.2, 465.95)
CAC LCx	40.2 (0.45, 192.65)
CAC RCA	97.3 (1.1, 428.85)

Values are presented as n (%).  
CAC coronary artery calcium; CSCT coronary calcium score CT scan; LAD left anterior descending; LCx left circumflex artery; LM left main; RCA right coronary artery

the automatically derived Agatston scores from LDCT as compared to CSCT scans in the per-patient analysis was 348.2 (IQR 64.45, 597.6) (Figure 2B). Based on the per vessel analysis, the highest variations in calcium score results were found in LM-LAD (99.7, IQR 15.25, 234.75, Supplementary Table S2). The agreement ( $\kappa$ ) between the results of the automatic Agatston scoring method in both CSCT and LDCT scans versus the gold standard was only 0.5 (95% CI 0.44-0.56). 29% of cases were assigned to the same risk category, and 93.6% of cases fell within one risk category (one risk category below or above the correct one). Using the automatic analysis method, 12.7% of patients were incorrectly assigned to the zero Agatston score category (Tables 5, 6B). The specificity, sensitivity, PPV and NPV were 100%, 81.7%, 100.0%, and 30.8%, respectively (Table 7).

*Manual assessment from LDCT scans vs gold standard CSCT* The total manually measured Agatston score on LDCT scans was significantly lower compared to CSCT scans (247.1 (IQR 32.4, 578.8) vs. 579.4 (IQR 139.4, 1103.8);  $P < .001$ ). The median difference between total Agatston scores in the per-patient analysis was 289.6 (IQR 55.5, 493.30) (Figure 2C). Similar to the automatic scoring method, the highest variation was

found in the LM-LAD, in the per vessel analysis (99.9, IQR 16.8, 217.95, Supplementary Table S2). The agreement ( $\kappa$ ) of calcium risk group analysis between the gold standard and the manual total Agatston scoring on LDCT scans was 0.58 (95% CI 0.52-0.63). 4.2% of cases were incorrectly assigned to the zero Agatston score category (Tables 5, 6B). The specificity, sensitivity, PPV and NPV were 100%, 95.5%, 100.0%, and 51.7%, respectively (Table 7). The inter-observer agreement on manual LDCT calcium scoring is summarized in Supplementary Table S3.

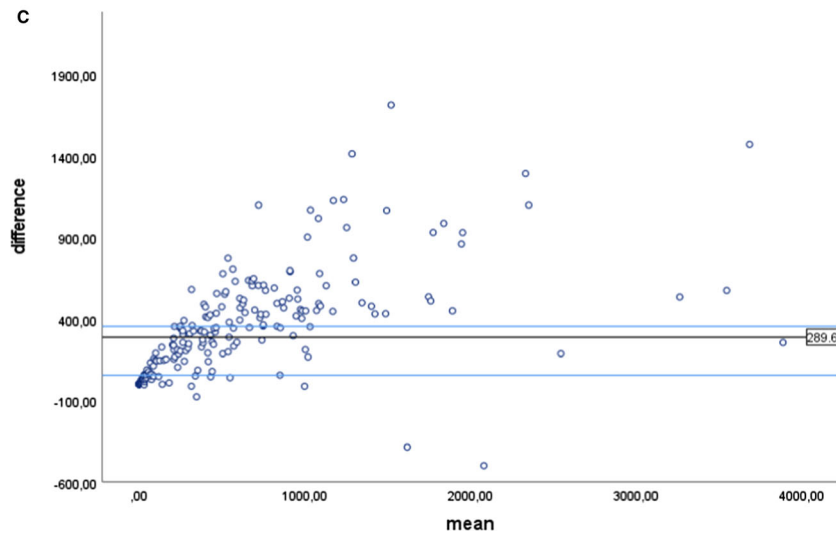
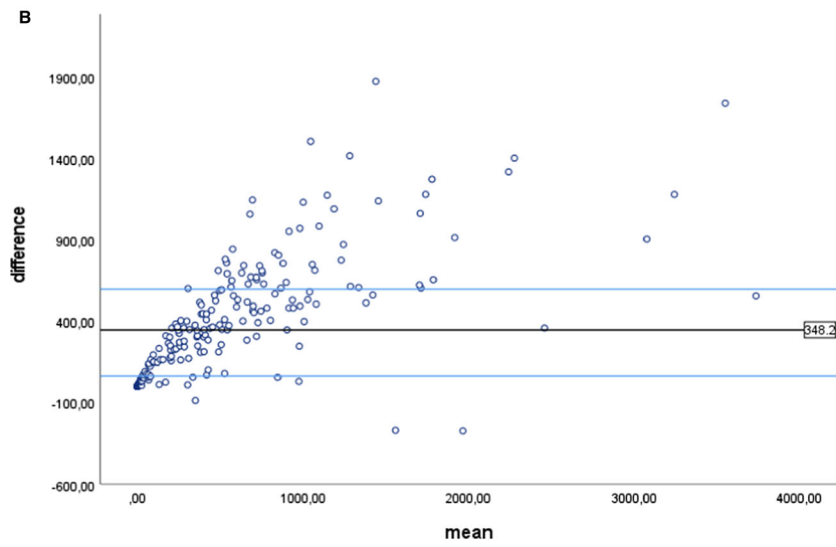
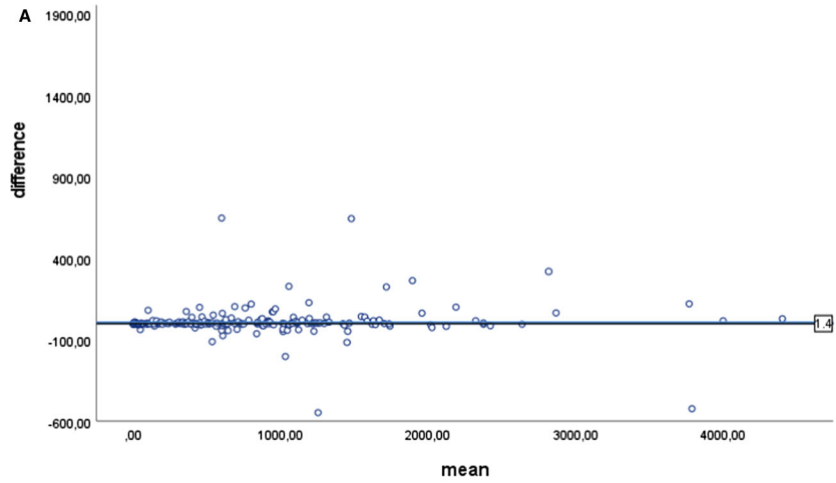
*Visual assessment of LDCT vs gold standard CSCT* Agreement ( $\kappa$ ) between visual scoring based on LDCT scans and the gold standard was 0.82 (95% CI 0.77–0.87). Compared to the gold standard, 74.2% of cases were assigned to the same category and 98.1% fell within one category (one risk category below or above the correct one). As compared to the automatic and manual method, the lowest number of cases were incorrectly assigned to the zero Agatston score category (3.2%) (Tables 6c, 7). Of the three evaluated calcium scoring methods from LDCT scans, visual scoring had the highest sensitivity and NPV (96.5%, 63.2%, respectively). The intra-observer agreement of visual calcium scoring from LDCT scans was high ( $\kappa = 0.94$ , 95% CI 0.92-0.96) and is summarized in Supplementary Table S4.

## DISCUSSION

The present study provides information about the applicability of a newly developed, clinically available, AI powered calcium scoring method, and visual assessment and traditional manual calcium scoring techniques using LDCT scans, compared to the results of the gold standard—manual calcium scoring on dedicated CSCT datasets. The results indicate that all three scoring methods correctly identify patients with CAC, as reflected in the high positive predictive values. Nevertheless, none of the scoring methods reliably excludes the presence of calcification, as reflected in the low negative predictive value. Visual calcium LDCT scoring provided the highest agreement with manual CSCT scoring.

### AI in calcium scoring from LDCT scans

A large and growing body of literature has assessed different methods of calcium scoring from LDCT scans. This is, to our knowledge, the first study which implements a new, automatic, commercially available AI powered calcium scoring technique on LDCT scans.<sup>10</sup> In addition to automatic scoring, we employed manual and visual scoring, and compared the results to



◀ **Figure 2.** Bland–Altman plots showing the median difference between Agatston score measured manually from CSCT scans and (A) Agatston score measured automatically from CSCT scans, (B) Agatston score measured automatically from LDCT scans, (C) Agatston score measured manually from LDCT scans.

the gold standard CSCT assessment. As a first step, we applied the automatic method on CSCT scans, which resulted in a comparable agreement in risk group classification as reported by Winkel et al ( $\kappa$  0.95 vs 0.89, respectively).<sup>10</sup> For LDCT calcium scores, however, the agreement dropped to 0.5. Despite this low agreement in risk group classification, in 93% of the scans the risk reclassification did not vary by more than one risk group. Moreover, the high specificity and positive predictive value of the automatic method indicated a correct identification of patients with CAC. Other studies in which automatic methods were applied to both CSCT scans and non-gated LDCT scans, outperformed the method we applied in our study. Recently, Zeleznik et al presented a deep learning method of calcium scoring which was applied on both gated and non-gated scans, with an overall agreement of 0.7.<sup>16</sup> Additionally, a fully automated CAC scoring method presented by Isgum et al demonstrated an agreement of 0.74 between LDCT scans and the gold standard.<sup>17</sup> The measurements performed by the automatic algorithm of Isgum et al were done on ECG-gated scans, using a DL algorithm that was trained for such gated scans. In contrast, the automatic method used in our study was not trained on non-gated scans.<sup>10</sup> Lack of ECG-triggering increases the amount of motion artifacts, decreases the accuracy of calcium detection and hence, potentially hampers quantification,<sup>18</sup> especially

when the DL algorithm was not trained on this type of data.<sup>19</sup> This may explain the lower agreement with the gold standard, as compared to the abovementioned studies.

It is interesting to note that in our study both automatic and manual calcium scoring from LDCT scans significantly underestimated the Agatston score. One explanation for this is that motion artifacts influence the number of voxels exceeding the 130 HU threshold.<sup>18</sup> In studies performed by Kaster et al and Mylonas et al, the calcium scoring threshold has been changed as low as 50 HU.<sup>20,21</sup> It should be underlined that as the HU threshold decreases, the false positive results increase due to higher noise levels. Moreover, the resulting calcium score is no longer an Agatston score by definition.<sup>8</sup> As reported by Mylonas et al, the highest agreement with the gold standard was achieved for a calcium threshold of 50 HU.<sup>21</sup> Nevertheless, these findings were not repeated elsewhere, and the value of the threshold was based on a very small sample size. Taking together, in our study the correlation between manual and automatic LDCT scoring as compared to the gold standard method was excellent. Nevertheless, systematic underestimation of the Agatston score resulted in a low overall agreement in risk classification.

Much of the current literature which focusses on automatic calcium assessment from LDCT scans highlights automatic methods of Agatston scoring. However, the lack of one, commonly used, validated protocol for LDCT scans, limits the application of Agatston scoring, which is a strictly defined method for calcium measurement.<sup>8</sup> Additionally, the majority of literature focusing on automatic methods, does not include the gold standard as a comparison. This may generally overestimate the performance of AI methods in calcium scoring.

**Table 5.** The agreement between automatic and visual scoring from CSCT scans and manual, automatic, and visual scoring from LDCT scans with a gold standard

	CSCT		LDCT		
	Automatic	Visual	Manual	Automatic	Visual
Weighted linear $\kappa$	0.95	0.88	0.59	0.50	0.82
95% CI	0.92-0.97	0.85-0.92	0.53-0.65	0.44-0.56	0.77-0.87
% of cases within the same category	91.0	82.1	35.2	29.5	74.2
% of cases within 1 category below or above the correct one	100	100	94.3	93.6	98.1
% of cases incorrectly assigned as 0 Agatston score	0.9	0	4.2	12.7	3.2



**Table 6.** Agreement in risk classification between (A) automatic, (B) manual and (c) visual assessment of LDCT scans and gold standard.

**(A)**

Automatic LDCT	Agatston score measured on CSCT						
	0	1-10	11-100	101-400	400-1 000	> 1 000	
0	12	9	14	4	0	0	39 (18.3%)
1-10	0	0	7	0	1	0	8 (3.8%)
11-100	0	0	6	16	7	0	29 (13.6%)
101-400	0	0	0	14	49	9	72 (33.8%)
401-1 000	0	0	0	0	12	34	46 (21.6%)
> 1 000	0	0	0	0	0	19	19 (8.9%)
	12 (5.6%)	9 (4.2%)	27 (12.7%)	34 (16.0%)	69 (32.4%)	62 (29.1%)	213

**(B)**

Manual LDCT	Agatston score measured on CSCT						
	0	1-10	11-100	101-400	400-1 000	> 1 000	
0	12	7	2	0	0	0	21 (9.9%)
1-10	0	2	13	2	0	0	17 (8.0%)
11-100	0	0	12	18	4	0	34 (16.0%)
101-400	0	0	0	14	49	4	67 (31.5%)
401-1 000	0	0	0	0	16	39	55 (25.8%)
> 1 000	0	0	0	0	0	19	19 (8.9%)
	12 (5.6%)	9 (4.2%)	27 (12.7%)	34 (16.0%)	69 (32.4%)	62 (29.1%)	213

**(C)**

Visual LDCT	Agatston score measured on CSCT						
	0	1-10	11-100	101-400	400-1 000	> 1 000	
0	12	5	1	1	0	0	19 (8.9%)
1-10	0	4	4	1	0	0	9 (4.2%)
11-100	0	0	20	8	0	0	28 (13.1%)
101-400	0	0	2	22	16	1	41 (19.2%)
401-1 000	0	0	0	2	53	14	69 (32.4%)
> 1 000	0	0	0	0	0	47	47 (22.1%)
	12 (5.6%)	9 (4.2%)	27 (12.7%)	34 (16.0%)	69 (32.4%)	62 (29.1%)	213

A: Weighted linear  $\kappa = 0.50$  (95% CI 0.44-0.56)

B: Weighted linear  $\kappa = 0.58$  (95% CI 0.52-0.63)

C: Weighted linear  $\kappa = 0.82$  (95% CI 0.77-0.87)

### Visual calcium scoring from LDCT scans

A visual analysis of calcium score was previously introduced by Einstein et al.<sup>9</sup> This simple method, repeated by others, has demonstrated good agreement with the gold standard.<sup>22-24</sup> In our study, of all applied methods, visual assessment of LDCT scan gained the highest agreement with CSCT calcium scoring. This is in line with the study of Einstein et al, who reported that

63% of visually estimated scores falls into the same category, while Engbers et al reported 71%.<sup>9,22</sup> In our study, 74.2% cases were correctly assigned to the same category and 94% did not vary by more than one risk category. Moreover, as compared to manual and automatic method, visual analysis yielded high sensitivity and good negative predictive value, which enables high-risk patients' detection.

**Table 7.** Sensitivity, specificity, PPV and NPV of CAC detectability on LDCT scans as compared to gold standard

	Manual LDCT	Automatic LDCT	Visual LDCT
Sensitivity	95.5	81.7	96.5
Specificity	100.0	100.0	100.0
PPV	100.0	100.0	100.0
NPV	57.1	30.8	63.2

LDCT low dose CT scan; NPV negative predictive value; PPV positive predictive value

### Comparison of patients' risk groups

The number of risk groups used in various studies complicates direct comparison between studies. For instance Zeleznik et al applied four risk groups, while the group of Isgum used a five risk group classification.<sup>16,17</sup> In our study, we decided to apply a six-risk group classification, which hampers a direct comparison with studies such as those by Zeleznik and Isgum. Our choice was justified by the fact that we aimed to evaluate how effective LDCT might be in the detection of high-risk group patients with an Agatston score > 1 000. Both automatic and manual assessment detected 19 out of 62 (30.6%) patients from the highest risk group. In terms of high-risk patient detection, visual analysis outperformed other techniques, correctly defining 47 out of 62 (75.8%) patients, which is comparable to the analysis conducted by Einstein et al. Importantly, both groups of Einstein and Engbers, used a six-point risk scale, which enables a comparison of the results with our study.<sup>9,22</sup>

### Clinical implications

According to Blaha et al, a coronary artery calcium score of zero is the most important negative risk predictor in asymptomatic and symptomatic patients.<sup>6,25</sup> Therefore, the greatest concern with LDCT scans is the underestimation of coronary calcium due to inability to detect small calcifications. In our study, low-risk patients were the most challenging group of patients to be identified, and this is reflected in a low sensitivity and negative predictive value of these tests. That was mostly pronounced in automatic scoring of LDCT, when 12.7% of patients were misclassified as zero Agatston score. Based on visual analysis, 3.2% of patients was misclassified as zero Agatston score despite having calcium on CSCT scan. This is lower than reported by the group of Einstein (22%), which might be explained by a relatively low amount of zero Agatston score scans in our study as compared to Einstein et al (5.6% vs 71.1%, respectively).<sup>9</sup>

Notwithstanding the clinical value of PET myocardial perfusion imaging, this method may underestimate the importance of the disease in patients with non-flow limiting coronary artery atherosclerosis, by leaving the incorrect impression of 'being healthy'. The additional information from LDCT scans about calcium signalizes the presence of atherosclerotic disease, which changes further patient management.<sup>23</sup> As already noticed and underlined by the Society of Cardiovascular Computed Tomography and Society of Thoracic Radiology, CAC should be reported even when found on non-contrast chest CT scans, however the optimal method of scoring is still not defined.<sup>11</sup> Based on our analysis, the visual scoring, which is a time-efficient method, demonstrated a good agreement with gold standard, and as shown by Engbers et al, and Patchett et al, may add a clinical value to MPI-PET scan.<sup>23,26</sup>

### Study limitations

This study has some limitations. First of all, LDCT scans were non-ECG triggered scans, characterized by a number of motion artifacts, which are a classic problem of these scans and significantly influences calcium measurement. Secondly, the study was performed using a relatively small sample size and further investigation is needed to confirm our results. Furthermore, patients were repositioned between CSCT and LDCT scans, and this might also account for discrepancy between results.<sup>27</sup> Additionally, the clinical AI algorithm we applied was not yet optimized for non-gated CT scans. Moreover, it was a single center study and all scans were acquired with the same protocol and identical scanners. On one hand this helped to unify the results and to draw conclusions, on the other hand the overall performance as compared with other scanning protocols and with different vendors remains unknown.

## CONCLUSIONS

In conclusion, visual calcium scoring from LDCT scans outperformed manual and automatic analysis and demonstrated the highest agreement with the reference CSCT. Within all three methods, automatic scoring gained the lowest sensitivity and NPV in calcium detectability. Nevertheless, each of abovementioned methods correctly defined patients with CAC. These results provide further support for the statement that CAC can be reported from LDCT scans, with visual scoring to be the most reliable method.

## NEW KNOWLEDGE GAINED

Visual assessment of calcium scores on LDCT scans outperforms both deep learning assisted and classic manual scoring methods and shows the best agreement with reference measurements on dedicated, ECG-triggered CSCT scans in the same patient.

## Disclosures

*Authors have nothing to disclose.*

## Open Access

*This article is licensed under a Creative Commons Attribution 4.0 International License, which permits use, sharing, adaptation, distribution and reproduction in any medium or format, as long as you give appropriate credit to the original author(s) and the source, provide a link to the Creative Commons licence, and indicate if changes were made. The images or other third party material in this article are included in the article's Creative Commons licence, unless indicated otherwise in a credit line to the material. If material is not included in the article's Creative Commons licence and your intended use is not permitted by statutory regulation or exceeds the permitted use, you will need to obtain permission directly from the copyright holder. To view a copy of this licence, visit <http://creativecommons.org/licenses/by/4.0/>.*

## References

1. Mach F, Baigent C, Catapano AL, et al. 2019 ESC/EAS guidelines for the management of dyslipidaemias: Lipid modification to reduce cardiovascular risk: The task force for the management of dyslipidaemias of the European Society of Cardiology (ESC) and European Atherosclerosis Society (EAS). *Eur Heart J* 2020;41:111-88. <https://doi.org/10.1093/eurheartj/ehz455>.
2. McClelland RL, Jorgensen NW, Budoff M, et al. 10-year coronary heart disease risk prediction using coronary artery calcium and traditional risk factors: Derivation in the MESA (Multi-Ethnic Study of Atherosclerosis) with validation in the HNR (Heinz Nixdorf Recall) study and the DHS (Dallas Heart Study). *J Am Coll Cardiol* 2015;66:1643-53. <https://doi.org/10.1016/j.jacc.2015.08.035>.
3. Budoff MJ, Shaw LJ, Liu ST, et al. Long-term prognosis associated with coronary calcification. Observations from a registry of 25,253 patients. *J Am Coll Cardiol* 2007;49:1860-70. <https://doi.org/10.1016/j.jacc.2006.10.079>.
4. Budoff MJ, Young R, Burke G, et al. Ten-year association of coronary artery calcium with atherosclerotic cardiovascular disease (ASCVD) events: The multi-ethnic study of atherosclerosis (MESA). *Eur Heart J* 2018;39:2401-8. <https://doi.org/10.1093/eurheartj/ehy217>.
5. Peng AW, Dardari ZA, Blumenthal RS, et al. Very high coronary artery calcium ( $\geq 1000$ ) and association with cardiovascular disease events, non-cardiovascular disease outcomes, and mortality: Results from MESA. *Circulation* 2021;143:1571-83. <https://doi.org/10.1161/CIRCULATIONAHA.120.050545>.
6. Blaha MJ, Cainzos-Achirica M, Greenland P, et al. Role of coronary artery calcium score of zero and other negative risk markers for cardiovascular disease: The multi-ethnic study of atherosclerosis (MESA). *Circulation* 2016. <https://doi.org/10.1161/CIRCULATIONAHA.115.018524>.
7. Lo-Kioeng-Shioe MS, Vavere AL, Arbab-Zadeh A, et al. Coronary calcium characteristics as predictors of major adverse cardiac events in symptomatic patients: Insights from the CORE320 multinational study. *J Am Heart Assoc* 2019. <https://doi.org/10.1161/JAHA.117.007201>.
8. Agatston AS, Janowitz WR, Hildner FJ, et al. Quantification of coronary artery calcium using ultrafast computed tomography. *J Am Coll Cardiol* 1990;15:827-32. [https://doi.org/10.1016/0735-1097\(90\)90282-T](https://doi.org/10.1016/0735-1097(90)90282-T).
9. Einstein AJ, Johnson LL, Bokhari S, et al. Agreement of visual estimation of coronary artery calcium from low-dose CT attenuation correction scans in hybrid PET/CT and SPECT/CT with standard Agatston score. *J Am Coll Cardiol* 2010;56:1914-21. <https://doi.org/10.1016/j.jacc.2010.05.057>.
10. Winkel DJ, Suryanarayana VR, Ali AM, et al. Deep learning for vessel-specific coronary artery calcium scoring: Validation on a multi-centre dataset. *Eur Heart J Cardiovasc Imaging* 2021. <https://doi.org/10.1093/ehjci/jeab119>.
11. Hecht HS, Cronin P, Blaha MJ, et al. 2016 SCCT/STR guidelines for coronary artery calcium scoring of noncontrast noncardiac chest CT scans: A report of the Society of Cardiovascular Computed Tomography and Society of Thoracic Radiology. *J Cardiovasc Comput Tomogr* 2017. <https://doi.org/10.1016/j.jcct.2016.11.003>.
12. Hecht HS, Cronin P, Blaha MJ, et al. 2016 SCCT/STR guidelines for coronary artery calcium scoring of noncontrast noncardiac chest CT scans: A report of the Society of Cardiovascular Computed Tomography and Society of Thoracic Radiology. *J Thorac Imaging* 2017;32:W54-66.
13. Thomas CK, Mühlenbruch G, Wildberger JE, et al. Coronary artery calcium scoring with multislice computed tomography: In vitro assessment of a low tube voltage protocol. *Invest Radiol* 2006;41:668-73. <https://doi.org/10.1097/01.rli.0000233324.09603.dd>.
14. Cohen J. A coefficient of agreement for nominal scales. *Educ Psychol Meas* 1960;20:37-46. <https://doi.org/10.1177/001316446002000104>.
15. Parikh R, Mathai A, Parikh S, et al. Understanding and using sensitivity, specificity and predictive values. *Indian J Ophthalmol* 2008;56:45-50. <https://doi.org/10.4103/0301-4738.37595>.
16. Zeleznik R, Foldyna B, Eslami P, et al. Deep convolutional neural networks to predict cardiovascular risk from computed tomography. *Nat Commun* 2021;12:715. <https://doi.org/10.1038/s41467-021-20966-2>.

17. Išgum I, de Vos BD, Wolterink JM, et al. Automatic determination of cardiovascular risk by CT attenuation correction maps in Rb-82 PET/CT. *J Nucl Cardiol* 2018;25:2133-42. <https://doi.org/10.1007/s12350-017-0866-3>.
18. van der Werf NR, Willemink MJ, Willems TP, et al. Influence of heart rate on coronary calcium scores: a multi-manufacturer phantom study. *Int J Cardiovasc Imaging* 2018;34:959-66. <https://doi.org/10.1007/s10554-017-1293-x>.
19. Xie X, Greuter MJW, Groen JM, et al. Can nontriggered thoracic CT be used for coronary artery calcium scoring A phantom study. *Med Phys* 2013. <https://doi.org/10.1118/1.4813904>.
20. Kaster TS, Dwivedi G, Susser L, et al. Single low-dose CT scan optimized for rest-stress PET attenuation correction and quantification of coronary artery calcium. *J Nucl Cardiol* 2015;22:419-28. <https://doi.org/10.1007/s12350-014-0026-y>.
21. Mylonas I, Kazmi M, Fuller L, et al. Measuring coronary artery calcification using positron emission tomography-computed tomography attenuation correction images. *Eur Heart J Cardiovasc Imaging* 2012;13:786-92. <https://doi.org/10.1093/ehjci/jes079>.
22. Engbers EM, Timmer JR, Mouden M, et al. Visual estimation of coronary calcium on computed tomography for attenuation correction. *J Cardiovasc Comput Tomogr* 2016. <https://doi.org/10.1016/j.jcct.2016.04.002>.
23. Patchett ND, Pawar S, Miller EJ. Visual identification of coronary calcifications on attenuation correction CT improves diagnostic accuracy of SPECT/CT myocardial perfusion imaging. *J Nucl Cardiol* 2017;24:711-20. <https://doi.org/10.1007/s12350-016-0395-5>.
24. Gaibazzi N, Suma S, Garibaldi S, et al. Visually assessed coronary and cardiac calcium outperforms perfusion data during scintigraphy in the prediction of adverse outcomes. *Int J Cardiol* 2020;312:123-8. <https://doi.org/10.1016/j.ijcard.2020.03.032>.
25. Sarwar A, Shaw LJ, Shapiro MD, et al. Diagnostic and prognostic value of absence of coronary artery calcification. *JACC Cardiovasc Imaging* 2009;2:675-88. <https://doi.org/10.1016/j.jcmg.2008.12.031>.
26. Engbers EM, Timmer JR, Ottervanger JP, et al. Prognostic value of coronary artery calcium scoring in addition to single-photon emission computed tomographic myocardial perfusion imaging in symptomatic patients. *Circ Cardiovasc Imaging* 2016. <https://doi.org/10.1161/CIRCIMAGING.115.003966>.
27. Willemink MJ, Vliegenthart R, Takx RAP, et al. Coronary artery calcification scoring with state-of-the-art CT scanners from different vendors has substantial effect on risk classification. *Radiology* 2014;273:695-702. <https://doi.org/10.1148/radiol.14140066>.
28. Pryor DB, Shaw L, Harrell FEJ, et al. Estimating the likelihood of severe coronary artery disease. *Am J Med* 1991;90:553-62.

**Publisher's Note** Springer Nature remains neutral with regard to jurisdictional claims in published maps and institutional affiliations.